

Ballistic Transport in High Electron Mobility Transistors

Jing Wang, *Student Member, IEEE*, and Mark Lundstrom, *Fellow, IEEE*

Abstract—A general ballistic FET model that was previously used for ballistic MOSFETs is applied to ballistic high electron mobility transistors (HEMTs), and the results are compared with experimental data for a sub-50 nm InAlAs–InGaAs HEMT. The results show that nanoscale HEMTs can be modeled as an intrinsic ballistic transistor with extrinsic source/drain series resistances. We also examine the “ballistic mobility” concept, a technique proposed for extending the drift-diffusion model to the quasi-ballistic regime. Comparison with a rigorous ballistic model shows that under low drain bias the ballistic mobility concept, although nonphysical, can be used to understand the experimental phenomena related to quasi-ballistic transport, such as the degradation of the apparent carrier mobility in short channel devices. We also point out that the ballistic mobility concept loses validity under high drain bias. The conclusions of this paper should be also applicable to other nanoscale transistors with high carrier mobility, such as carbon nanotube FETs and strained silicon MOSFETs.

Index Terms—Ballistic transport, high electron mobility transistors (HEMTs), mobility, semiconductor device modeling.

I. INTRODUCTION

As the channel lengths of integrated circuit transistors continue to shrink to the sub-50 nm regime, there is more and more interest in device behavior and performance at the ballistic limit [1]–[4]. In silicon MOSFETs, due to the relatively low mobility of the inversion layer electrons ($\sim 100 \text{ cm}^2/\text{V} \cdot \text{s}$ at room temperature), the device performance is still below 50% of its ballistic limit [5]. On the other hand, high electron mobility transistors (HEMTs), which have extremely high electron mobility ($\sim 10,000 \text{ cm}^2/\text{V} \cdot \text{s}$ at room temperature), should operate near the ballistic limit [2], [6]. Understanding ballistic transport in sub-50 nm HEMTs [7], [8] is, therefore, important for both device modeling and for the explanation of experimental results [6].

In the ballistic or quasi-ballistic regimes, the conventional device equations based on the drift-diffusion theory are not valid, and consequently a new theory of ballistic transistors is needed. Natori first developed this theory for silicon MOSFETs [1], and it has been extended to a general ballistic model [9], [10]. Recently, Shur has also introduced the concept of “ballistic

mobility” in order to capture ballistic effects in short channel HEMTs while retaining a drift-diffusion formalism [6]. The motivation of this approach is to retain a familiar description of devices, but mobility is not a physically meaningful concept in the quasi-ballistic regime. Our objective in this paper is not to take a position on whether or not the ballistic mobility concept should be used but, rather, to clarify when it does and does not work. We first apply a rigorous ballistic model to HEMTs and compare the results with experimental data for a sub-50 nm device [7]. The comparison shows that modern HEMTs can be modeled as a ballistic device with series resistances. We then compare the results of the ballistic mobility method with those of the rigorous ballistic model to examine the validity of the ballistic mobility method. We find that it can be used under low drain bias, but not, in a short channel HEMT, under high drain bias.

II. GENERAL BALLISTIC FET MODEL

The general ballistic FET model is a simple analytical model that correctly captures quantum confinement, two-dimensional (2-D) electrostatics, and bias-charge self-consistency in ballistic FETs [9], [10]. It generalizes Natori’s model [1] by treating 2-D electrostatics and by properly treating the two-dimensional (1-D) electrostatics—even in the quantum capacitance limit (where the gate insulator capacitance is much greater than the semiconductor (or quantum) capacitance [2], [9], [11]). Fig. 1 summarizes the essential aspects of the general ballistic model. It consists of three capacitors (C_G , C_S and C_D), which represent the effects of the three terminals (the gate, source and drain) on the potential at the top of the barrier [9]. The height of the potential barrier between the source and drain is

$$U_{\text{TOP}} = -q \left[\left(\frac{C_G}{C_G + C_D + C_S} \right) V_G + \left(\frac{C_D}{C_G + C_D + C_S} \right) \times V_D + \left(\frac{C_S}{C_G + C_D + C_S} \right) V_S \right] + \frac{q^2 N_{\text{mobile}}}{(C_G + C_D + C_S)} \quad (1)$$

where the first three terms, the Laplace solution, describe the influence of the three terminals and the last term, the charging energy, describes the effect of the mobile charge at the top of the barrier. (For a well-designed MOSFET, $C_G \gg C_D$, C_S , and the potential is primarily controlled by the gate voltage.) Knowing the bottom of the band at the top of the barrier, the mobile charge N_{mobile} is computed by filling the $+k$ states according to the source Fermi level (set by the source voltage), and the $-k$ states according to the drain Fermi level (set by the drain voltage). The process of computing the potential at the top of the barrier from (1), then updating the mobile charge there

Manuscript received February 5, 2003; revised May 5, 2003. This work was supported by the Defense University Research Initiative in Nanotechnology funded by the Army Research Office and monitored by Dr. D. Woolland, and by the MARCO Focused Research Center on Materials, Structures, and Devices, which is funded at the Massachusetts Institute of Technology, in part by MARCO under Contract 2001-MT-887 and DARPA by Grant MDA972-01-1-0035. The review of this paper was arranged by Editor C.-P. Lee.

The authors are with the School of Electrical and Computer Engineering, Purdue University, West Lafayette, IN 47907 USA (e-mail: jingw@purdue.edu).

Digital Object Identifier 10.1109/TED.2003.814980

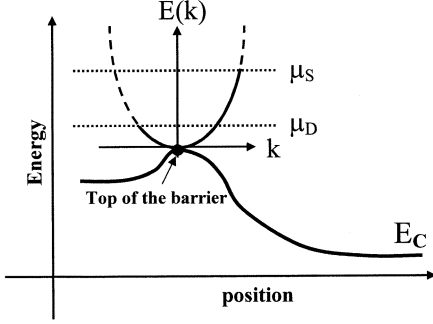


Fig. 1. Illustration of the essential features of the general, ballistic transistor model. μ_S is the source Fermi level and μ_D is the drain Fermi level.

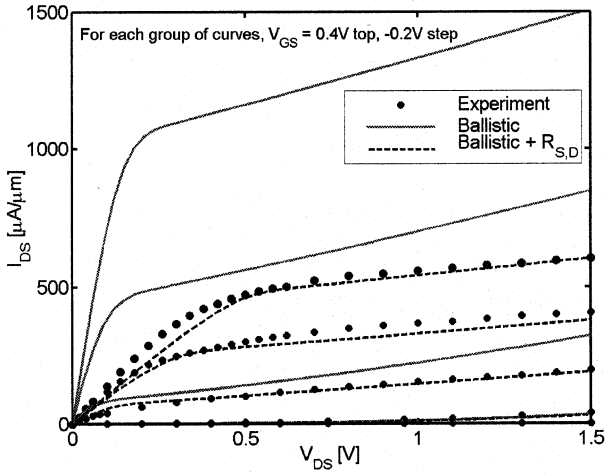


Fig. 2. Comparison of the simulated ballistic I - V with experimental data. The solid lines are for the intrinsic ballistic device, the dashed lines are for the extrinsic device (with extrinsic source/drain series resistances $R_S = R_D = 400 \Omega \cdot \mu\text{m}$) and the circles are for experiment data (obtained from [7, p. 1696, Fig. 6(b)], $L_g = 30 \text{ nm}$, $L_{\text{side}} = 260 \text{ nm}$).

continues until convergence is achieved after which the drain current is readily evaluated from the known populations of the $+k$ and $-k$ states. For a detailed discussion of the model, see [9]. In this work, we extended the model to include electrons in multiple subbands, because the channel layer of sub-50-nm HEMTs [7], [8] is usually much thicker than that of 10-nm scale silicon MOSFETs or carbon nanotube transistors, for which the one-subband assumption adopted in [9], [10] is adequate.

Using the general ballistic model, we simulated a recently reported 30-nm InP-based InAlAs-InGaAs HEMT [7]. (The Matlab script for the calculation is available from the authors.) The current-voltage curves are plotted in Fig. 2. We treated the intrinsic device as a ballistic transistor with a 13-nm-thick InAlAs gate insulator layer and a 15-nm-thick InGaAs channel (see [7, p. 1694, Fig. 1] for details of the device geometry); extrinsic series resistances of $R_S = R_D = 400 \Omega \cdot \mu\text{m}$ were also included. (In the simulation of the intrinsic device, we assumed that the source/drain capacitances $C_S = C_D = 0.1 \cdot C_G$, which gives us the best agreement with experiment data.) The simulated current-voltage (I - V) curves of the extrinsic device (dashed lines) show good agreement with the measured data (circles), which are much lower than the ballistic limit of the intrinsic device (solid lines). Consequently, we can conclude

that in the sub-50-nm regime, carrier transport within the intrinsic HEMTs is almost ballistic, but the source/drain series resistances lower the current substantially and are, therefore, important for the calculation of current characteristics. A similar conclusion was reached by Solomon and Laux in [2].

III. BALLISTIC MOBILITY METHOD

In [6], Shur introduced the concept of ballistic mobility μ_B and provided an expression valid for nondegenerate conditions (see also [12]). The motivation is to retain the *form* of the traditional FET model (where mobility is a physically well-defined concept) in the quasi-ballistic regime, where mobility loses its physical basis. In the quasi-ballistic regime, the mobility used in the conventional device equations is replaced by an effective mobility μ_{eff} , which is calculated by Mathiessen's rule as [6]

$$\frac{1}{\mu_{\text{eff}}} = \frac{1}{\mu_B} + \frac{1}{\mu_0} \quad (2)$$

where μ_0 is the real, physical mobility in a long-channel (scattering-dominated) device.

In the remainder of this section, we first derive an expression for μ_B under arbitrary levels of carrier degeneracy and then examine the validity of the ballistic mobility method under both low and high drain biases.

A. Derivation of the Ballistic Mobility μ_B

In the conventional device equations, the drain current under low drain bias can be expressed as [13]

$$\frac{I_{DS}}{W} = Q_i(0) \mu \frac{V_{DS}}{L} \quad (3)$$

where $Q_i(0)$ is the sheet electron density at the beginning of the channel and other symbols have their common meanings. On the other hand, the ballistic drain current can be obtained from [14] (see [14, eq. 6, p. 483], with the backscattering coefficient $r = 0$) as

$$\frac{I_{DS}}{W} = Q_i(0) \left[v_T \frac{\mathfrak{S}_{1/2}(\eta_F)}{\mathfrak{S}_0(\eta_F)} \right] \times \frac{\frac{1 - \mathfrak{S}_{1/2}(\eta_F - U_D)}{\mathfrak{S}_{1/2}(\eta_F)}}{\frac{1 + \mathfrak{S}_0(\eta_F - U_D)}{\mathfrak{S}_0(\eta_F)}} \quad (4)$$

where $v_T = \sqrt{2k_B T / \pi m^*}$ is the unidirectional thermal velocity of nondegenerate electrons, and the term in brackets is the unidirectional thermal velocity under general conditions. The function $\mathfrak{S}_i(x)$ is the Fermi-Dirac integral $U_D = V_{DS} / (k_B T / q)$ and $\eta_F = (E_F - E_{C0}) / k_B T$, where E_F is the source Fermi level and E_{C0} is the first subband level for electrons at the beginning of the channel. Under low drain bias ($V_{DS} \ll k_B T / q$), $U_D \rightarrow 0$, so (4) can be simplified as

$$\begin{aligned} \frac{I_{DS}}{W} &= \frac{Q_i(0) v_T}{2 \mathfrak{S}_0(\eta_F)} \frac{\partial \mathfrak{S}_{1/2}(\eta_F)}{\partial \eta_F} U_D \\ &= \frac{Q_i(0) v_T}{2 \mathfrak{S}_0(\eta_F)} \mathfrak{S}_{-1/2}(\eta_F) \frac{q V_{DS}}{k_B T}. \end{aligned} \quad (5)$$

By equating (3) and (5), we can define a nonphysical ballistic mobility μ_B as

$$\mu_B = \frac{qL}{\pi m^* v_T} \frac{\mathfrak{S}_{-1/2}(\eta_F)}{\mathfrak{S}_0(\eta_F)}. \quad (6)$$

Under nondegenerate conditions, $\mathfrak{S}_{-1/2}(\eta_F) = \mathfrak{S}_0(\eta_F) = e^{\eta_F}$, so $\mu_B = qL/(\pi m^* v_T)$, which is the same as Shur's expression in [6]. (Note that Shur expressed his results in terms of the thermal average speed $v_{Th} = \sqrt{8k_B T/\pi m^*}$, while we express the same result in terms of the unidirectional thermal velocity, $v_T = \sqrt{2k_B T/\pi m^*}$.) At zero temperature, $\mu_B = 2qL/(\pi m^* v_f)$, where v_f is the Fermi velocity of electrons. Finally, by inserting (6) into (3), we can use the conventional device equations to calculate the ballistic current under low drain bias. (Note, however, that this derivation is valid under low drain bias only.)

B. Examination of the Validity of the Ballistic Mobility Method

1) *Device Structure and Methodology*: In this section, we compare the results of the ballistic mobility method with those of the general ballistic model described in Section II. The device structure is an intrinsic, ballistic, single-gate AlGaAs–GaAs HEMT with a 10-nm-thick gate insulator. (In a ballistic simulation, the current is independent of the channel length.) For simplicity, we assume that the body of the device is thin enough so that the one-subband approximation can be adopted. (Since the main purpose for this part of the work is to compare the two transport models, the one-subband assumption simplifies the calculation and enables us to make a clear comparison between the two models.) We also assume that there is no series resistance and no 2-D electrostatic effects (i.e., DIBL). This ideal device structure is simulated by both methods under low and high drain biases, respectively. In the ballistic mobility simulation, the conventional device equations [13] with *velocity saturation* are adopted, and the effective mobility is equal to the ballistic mobility since this is a ballistic simulation.

In the conventional device equations, the channel electron density is given by $Q_i(0) = C_{\text{eff}}(V_{GS} - V_T)$, where V_T is the threshold voltage. In this case, $C_{\text{eff}} = C_I C_Q / (C_I + C_Q)$, where C_I is the gate insulator capacitance and C_Q is the semiconductor (or quantum) capacitance [9]–[11], which is equal to $q^2 D_0$ at zero temperature for the one-subband assumption (here D_0 is the density of states for the confined 2-D electron gas in the channel). In the calculation of the ballistic mobility using (6) we need to know the degeneracy factor $\mathfrak{S}_{-1/2}(\eta_F)/\mathfrak{S}_0(\eta_F)$, which can be extracted from the results of the general ballistic model.

2) *Low Drain Bias*: Under low drain bias, we define the channel conductance as

$$g_{DS} = \left. \frac{\partial I_{DS}}{\partial V_{DS}} \right|_{V_{DS}=0} \quad (7)$$

which is plotted versus gate voltage in Fig. 3. Fig. 3 shows that the ballistic mobility method agrees quite well with the general ballistic model for the calculation of the ballistic channel conductance under low drain bias, as expected from the derivation in Section III-A.

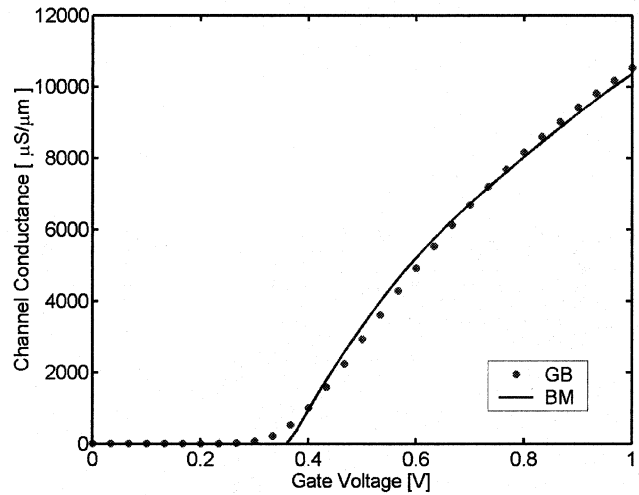


Fig. 3. Simulated channel conductance for the ballistic AlGaAs–GaAs HEMT. The solid line is from the ballistic mobility (BM) method, and the circles are from the general ballistic (GB) model. The threshold voltage used in the ballistic mobility method is extracted from the results of the general ballistic model.

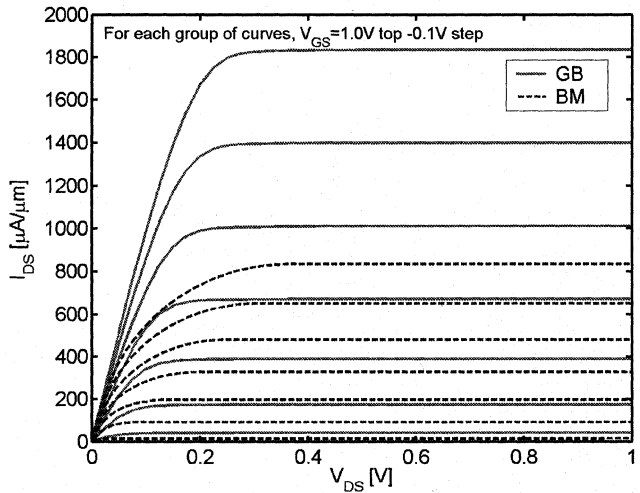


Fig. 4. Simulated I_{DS} – V_{DS} curves for the ballistic AlGaAs–GaAs HEMT. The dashed lines are from the ballistic mobility (BM) method, and the solid lines are from the general ballistic (GB) model. The saturation velocity used in the ballistic mobility simulation is equal to the unidirectional thermal velocity \bar{v}_T and the threshold voltage used in the ballistic mobility method is extracted from the results of the general ballistic model.

Another question we consider is whether Mathiessen's rule [as in (2)] can be used in the quasi-ballistic regime (where there is some scattering and the physical mobility μ_0 is finite). By comparing the ballistic mobility method with the quasi-ballistic transport theory [15], [16], we find that under low drain bias, Mathiessen's rule is still valid (see the Appendix for details). In summary, with the ballistic mobility of (6) and Mathiessen's rule in (2), we can use the conventional device equations to treat ballistic/quasi-ballistic transport under *low* drain bias.

3) *High Drain Bias*: The simulated I_{DS} – V_{DS} curves plotted in Fig. 4 show that although the ballistic mobility method agrees with the general ballistic model under low drain bias, it substantially underestimates the current under high drain bias. The derivation in Section III-A explains why the

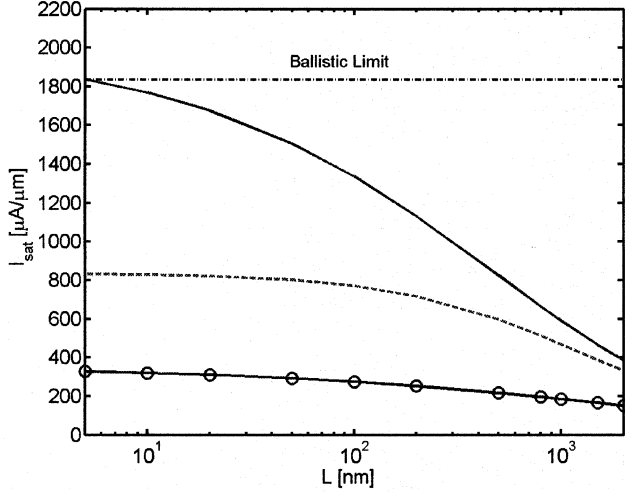


Fig. 5. Simulated saturation current versus channel length curves for the quasi-ballistic (the real, physical mobility has finite value, $\mu_0 = 8,000 \text{ cm}^2/\text{V} \cdot \text{s}$) AlGaAs-GaAs HEMT. ($V_{GS} = V_{DS} = 1.0 \text{ V}$) The saturation current is estimated by the conventional device equation with (a) the physical mobility ($\mu_0 = 8,000 \text{ cm}^2/\text{V} \cdot \text{s}$) and the ballistic saturation velocity \bar{v}_T (solid line). (b) The effective mobility calculated from (2) and the ballistic saturation velocity \bar{v}_T (dashed line). (c) The physical mobility and the saturation velocity in bulk GaAs ($v_{\text{sat}} = 8.4 \times 10^4 \text{ m/s}$ at $T = 300 \text{ K}$ [18]) (solid line with circles).

ballistic mobility approach works under low drain bias, but why does it fail under high drain bias?

Current is the product of charge and velocity. Under low drain bias, the velocity is proportional to the electric field (which is proportional to the drain bias). The ballistic mobility method works well since it gives the proper relation between the velocity and electric field, as derived in Section III-A. Under high drain bias, however, the electron velocity saturates—both in the ballistic regime [17] and when scattering dominates. In the ballistic regime, the saturation velocity (under high drain bias) can be evaluated from (4) as

$$I_{\text{sat}} = WQ_i(0)\bar{v}_T = WQ_i(0) \left[v_T \frac{\mathfrak{S}_{1/2}(\eta_F)}{\mathfrak{S}_0(\eta_F)} \right]. \quad (8)$$

On the other hand, in the conventional equations, the saturation current can be expressed as [13]

$$I_{\text{sat}} = WQ_i(0)v_{\text{sat}} \frac{\sqrt{1 + \frac{2\mu_0(V_{GS}-V_T)}{(mv_{\text{sat}}L)}} - 1}{\sqrt{1 + \frac{2\mu_0(V_{GS}-V_T)}{(mv_{\text{sat}}L)}} + 1} \quad (9)$$

where $m = 1 + C_{dm}/C_I$, and C_{dm} is the maximum depletion-layer capacitance. When the channel length, L , approaches zero (or the physical mobility μ_0 approaches infinity), μ_0/L approaches infinity and (9) can, therefore, be simplified as

$$I_{\text{sat}} = WQ_i(0)v_{\text{sat}}. \quad (10)$$

Thus, by replacing the bulk saturation velocity v_{sat} with the unidirectional thermal velocity \bar{v}_T , we can use a conventional $I_{DS}-V_{DS}$ equation to estimate the ballistic limit of the saturation current, as shown in Fig. 5. The use of the ballistic mobility,

which is derived under low drain bias, will lower the mobility unphysically under high drain bias and consequently underestimate the saturation current.

Fig. 5 shows the saturation current calculated by the conventional equation at different channel lengths. With the use of the physical mobility ($\mu_0 = 8,000 \text{ cm}^2/\text{V} \cdot \text{s}$) and the correct ballistic saturation velocity \bar{v}_T (solid line), the conventional equation gives the proper ballistic saturation current as the channel length approaches zero. If we substitute the effective mobility calculated from (2) for the physical mobility and still use \bar{v}_T as the saturation velocity (dashed line), the saturation current is less than 50% of the ballistic limit. If we keep the physical mobility but replace \bar{v}_T by the saturation velocity in bulk GaAs ($v_{\text{sat}} = 8.4 \times 10^4 \text{ m/s}$ at $T = 300 \text{ K}$ [18]), the saturation current is also substantially underestimated (solid line with circles). We conclude, therefore, that a good estimation of saturation current (by the conventional equation) in the ballistic regime requires the use of both a correct mobility and a proper saturation velocity, which are determined by the physics of ballistic transport.

IV. DISCUSSION

Mobility is a concept used when scattering dominates, but in the quasi-ballistic regime, it loses its physical meaning. The introduction of a nonphysical ballistic mobility (together with Mathiessen's rule) allows conventional FET $I-V$ equations to be used under low drain bias. The apparent mobility one deduces from experiments at low field is defined by (2). When the channel is long, the ballistic mobility is much larger than the physical mobility and the apparent mobility is equal to the physical mobility. When the channel is very short compared to the electron's mean free path, however, the ballistic mobility will be much smaller than the physical mobility, and the mobility one measures is the ballistic mobility not the physical mobility. That is why the measured apparent mobility is reduced in very short channel devices. This effect is not important in silicon devices because the mobility is relatively low, but it is significant in the devices with very high electron mobility, such as HEMTs (observed by Shur [6]), strained silicon MOSFETs [19] and carbon nanotube FETs [20]. Understanding the physics of quasi-ballistic transport is critical for interpreting the measurement of carrier mobility in short channel devices.

Much has been invested in the development of drift-diffusion based compact models for circuit simulation. Such models are the link between the device and circuit and system levels. It would be useful if the investment in the development of such models could be leveraged so that they could be extended to the ballistic and quasi-ballistic regimes. The ballistic mobility concept is a partial solution that works under low drain bias. It allows us to retain the traditional FET model by redefining the mobility in terms of a nonphysical effective mobility. Unfortunately, the results of this paper show that this approach only works for low drain bias. At this time it is still unclear as to whether or not a clean technique to extend traditional FETs can be developed or if a new class of compact models will have to be developed.

V. SUMMARY

In this paper, we applied a rigorous ballistic FET model (previously used for ballistic MOSFETs) to ballistic HEMTs and, by comparing the results to experimental data for a sub-50-nm HEMT, we showed that modern-day HEMTs can be described as an intrinsic ballistic device with extrinsic source/drain series resistances. In contrast, silicon MOSFETs operate at less than one half of the ballistic limit because of the low inversion layer mobility. We also extended Shur's ballistic mobility method to the degenerate case and examined its validity by comparing it to the rigorous ballistic model. We observed that the ballistic mobility method is valid when the drain bias is *low*. Consequently, it can be a good way for us to understand the degradation of the measured apparent mobility in short channel HEMTs as well as other transistors with very high carrier mobility, such as carbon nanotube FETs and strained silicon MOSFETs. Unfortunately, the straightforward extension of traditional FET models to the ballistic/quasi-ballistic regime through the use of a nonphysical ballistic mobility fails for high drain bias. Since modern-day HEMTs operate near the ballistic limit, it will be important to develop circuit models that behave properly in the ballistic limit.

APPENDIX

From the scattering theory of the MOSFET [15], there is a simple relationship between the drain current in the presence of scattering and its ballistic limit. Under low drain bias and *nondegenerate* conditions

$$I_{DS} = \frac{\lambda}{\lambda + L} I_{\text{ballistic}} \quad (\text{A1})$$

where λ is the mean-free-path for carriers, and L is the channel length. Under nondegenerate condition, according to the Einstein relation, the electron mobility is $\mu_0 = (q/k_B T) D_n$, where $D_n = (v_T \lambda)/2$ is the diffusion coefficient. Using these expressions, we find

$$\mu_0 = \frac{q v_T \lambda}{2 k_B T} = \frac{q \lambda}{\pi m^* v_T}. \quad (\text{A2})$$

Using (6) for the ballistic mobility under nondegenerate condition $\mu_B = qL/(\pi m^* v_T)$ we find

$$\frac{\lambda}{\lambda + L} = \frac{\mu_0}{\mu_0 + \mu_B}. \quad (\text{A3})$$

Under low drain bias, the ballistic current from (3) can be expressed in terms of the ballistic mobility as

$$I_{\text{ballistic}} = W Q_i(0) \mu_B \frac{V_{DS}}{L}. \quad (\text{A4})$$

By inserting (A3) and (A4) into (A1), we obtain the drain current in the presence of scattering as

$$I_{DS} = \frac{\mu_0 \mu_B}{\mu_0 + \mu_B} W Q_i(0) \frac{V_{DS}}{L} \quad (\text{A5})$$

so $\mu_{\text{eff}} = \mu_0 \cdot \mu_B / (\mu_0 + \mu_B)$, and Mathiessen's rule is valid. Note that this derivation is based on the nondegenerate assumption. Under degenerate condition, (A1) needs to be modified as

$$I_{DS} = \frac{\alpha \lambda}{\alpha \lambda + L} I_{\text{ballistic}} \quad (\text{A6})$$

and the value of α can be determined as the following.

At the diffusive limit ($L \gg \lambda$), we find that $I_{DS} = (\alpha \lambda / L) I_{\text{ballistic}}$. The ballistic current under low drain bias is given by (5), so we can express the current as

$$I_{DS} = \frac{\alpha \lambda W Q_i(0) v_T}{2L} \frac{q V_{DS}}{k_B T} \frac{\mathfrak{S}_{-1/2}(\eta_F)}{\mathfrak{S}_0(\eta_F)}. \quad (\text{A7})$$

The relationship between the mean-free-path λ and the physical mobility μ_0 is [14]

$$\lambda = \left(\frac{2 \mu_0 k_B T}{v_T q} \right) \cdot \frac{[\mathfrak{S}_0(\eta_F)]^2}{\mathfrak{S}_{-1}(\eta_F) \mathfrak{S}_{1/2}(\eta_F)}. \quad (\text{A8})$$

By inserting (A8) into (A7), we obtain

$$I_{DS} = \alpha \frac{\mathfrak{S}_{-1/2}(\eta_F) \mathfrak{S}_0(\eta_F)}{\mathfrak{S}_{-1}(\eta_F) \mathfrak{S}_{1/2}(\eta_F)} W Q_i(0) \mu_0 \frac{V_{DS}}{L}. \quad (\text{A9})$$

At the diffusive limit, (A9) should be the same as the conventional equation (see (3) in Section III-A), so we get

$$\alpha = \frac{\mathfrak{S}_{-1}(\eta_F) \mathfrak{S}_{1/2}(\eta_F)}{\mathfrak{S}_{-1/2}(\eta_F) \mathfrak{S}_0(\eta_F)}. \quad (\text{A10})$$

Under the nondegenerate condition, $\alpha = 1$, and (A6) is the same as (A1). At zero temperature, $\alpha = 2/3$. This result is consistent with the quasi-ballistic transport theory at zero temperature [16] (note the L_0 in [16, p. 62 (2.2.2)] should be equal to $2\lambda/3$ according to its definition $D_n = v_f L_0 / \pi$).

Finally, having found the expression for the coefficient α in (A6), we can use (A6) and (A10) to verify that Mathiessen's rule is also valid under the degenerate condition. [The procedure for the calculation is the same as that for nondegenerate condition (A1)–(A5)].

ACKNOWLEDGMENT

The authors would like to thank Prof. M. S. Shur at Rensselaer Polytechnic Institute, R. Tsai and D. Streit at Northrop Grumman Space Technology, and A. Javey at Stanford University for their sincere help with this paper.

REFERENCES

- [1] K. Natori, "Ballistic metal-oxide-semiconductor field effect transistor," *J. Appl. Phys.*, vol. 76, no. 8, pp. 4879–4890, Oct. 1994.
- [2] P. M. Solomon and S. E. Laux, "The ballistic FET: Design, capacitance and speed limit," in *IEEE Int. Electron. Dev. Meeting (IEDM), Tech. Dig.*, Dec. 3–5, 2001, pp. 95–98.
- [3] F. Assad, Z. Ren, D. Vasilevski, S. Datta, and M. S. Lundstrom, "On the performance limits for Si MOSFETs: A theoretical study," *IEEE Trans. Electron Devices*, vol. 47, pp. 232–240, Jan. 2000.
- [4] Z. Ren, R. Venugopal, S. Datta, M. Lundstrom, D. Jovanovic, and J. G. Fossum, "The ballistic nanotransistor: A simulation study," in *IEDM Tech. Dig.*, Dec. 10–13, 2000, pp. 715–718.
- [5] A. Lochtefeld and D. A. Antoniadis, "On experimental determination of carrier velocity in deeply scaled NMOS: how close to the thermal limit?," *IEEE Electron Device Lett.*, vol. 22, pp. 95–97, Feb. 2001.

- [6] M. S. Shur, "Low ballistic mobility in submicron HEMT's," *IEEE Electron Device Lett.*, vol. 23, pp. 511–513, Sept. 2002.
- [7] T. Suemitsu, H. Yokoyama, T. Ishii, T. Enoki, G. Meneghesso, and E. Zanoni, "30 nm two-step recess gate InP-based InAlAs/InGaAs HEMT's," *IEEE Trans. Electron Devices*, vol. 49, pp. 1694–1700, Oct. 2002.
- [8] Y. Yamashita, A. Endoh, K. Shinohara, T. Matsui, S. Hiyamizu, and T. Mimura, "Pseudomorphic $\text{In}_{0.52}\text{Al}_{0.48}\text{As}/\text{In}_{0.7}\text{Ga}_{0.3}\text{As}$ HEMT's with an ultrahigh f_T of 562 GHz," *IEEE Electron Device Lett.*, vol. 23, pp. 573–575, Oct. 2002.
- [9] A. Rahman, J. Guo, S. Datta, and M. Lundstrom, "Theory of ballistic nanotransistors," *IEEE Trans. Electron Devices*, vol. 50, Sept. 2003, to be published.
- [10] J. Guo, S. Datta, M. Lundstrom, M. Brink, P. McEuen, A. Javey, H. Dai, H. Kim, and P. McIntyre, "Assessment of silicon MOS and carbon nanotube FET performance limits using a general theory of ballistic transistors," in *IEDM Tech. Dig.*, Dec. 9–11, 2002, pp. 711–714.
- [11] S. Luryi, "Quantum capacitance devices," *Appl. Phys. Lett.*, vol. 52, pp. 501–503, Feb. 1988.
- [12] A. A. Kastalsky and M. S. Shur, "Conductance of small semiconductor devices," *Solid State Commun.*, vol. 39, no. 6, pp. 715–718, 1981.
- [13] Y. Yaur and T. H. Ning, *Fundamentals of Modern VLSI Devices*. Cambridge, UK: Cambridge Univ. Press, 1998.
- [14] A. Rahman and M. Lundstrom, "A compact scattering model for the nanoscale double-gate MOSFET," *IEEE Trans. Electron Devices*, vol. 49, pp. 481–489, Mar. 2002.
- [15] M. Lundstrom, "Elementary scattering theory of the Si MOSFET," *IEEE Electron Device Lett.*, vol. 18, pp. 361–363, July 1997.
- [16] S. Datta, *Electronic Transport in Mesoscopic Structures*. Cambridge, UK: Cambridge Univ. Press, 1999.
- [17] M. Lundstrom and Z. Ren, "Essential physics of carrier transport in nanoscale MOSFET's," *IEEE Trans. Electron Devices*, vol. 49, pp. 133–141, Jan. 2002.
- [18] M. Lundstrom, *Fundamentals of Carrier Transport*. Cambridge, UK: Cambridge Univ. Press, 2000.
- [19] K. Rim, S. Narasimha, M. Longstreet, A. Mocuta, and J. Cai, "Low field mobility characteristics of Sub-100 nm unstrained and strained Si MOSFET's," in *IEDM Tech. Dig.*, Dec. 9–11, 2002, pp. 43–46.
- [20] A. Javey, *Personal Commun.*: Stanford Univ., 2002.



Jing Wang (S'03) was born in China in 1979. He received the B.E. degree from the Department of Electronic Engineering, Tsinghua University, Beijing, China, in 2001. Currently he is pursuing the Ph.D. degree student with the School of Electrical and Computer Engineering, Purdue University, West Lafayette, IN.

His research interests center on the theory and simulation of nanometer scale electronic devices, which includes the modeling and design of nanoscale MOSFETs and post-CMOS transistors, as well as the transport theory for HEMTs.



Mark Lundstrom (S'72–M'74–SM'80–F'94) received the B.E.E. and M.S.E.E. degrees from the University of Minnesota, Minneapolis, in 1973 and 1974, respectively.

He joined the faculty of Purdue University, West Lafayette, IN, upon completing his doctorate on the West Lafayette campus in 1980. Before attending Purdue, he was with Hewlett-Packard Corporation, where he worked on integrated circuit process development and manufacturing. He is the Scifres Distinguished Professor of Electrical and Computer

Engineering at Purdue University, where he also directs the NSF Network for Computational Nanotechnology. His current research interests center on the physics of semiconductor devices, especially nanoscale transistors. His previous work includes studies of heterostructure devices, solar cells, heterojunction bipolar transistors and semiconductor lasers. During the course of his Purdue career, he has served as Director of the Optoelectronics Research Center and Assistant Dean of the Schools of Engineering.

Dr. Lundstrom is a fellow of the American Physical Society and the recipient of several awards for teaching and research—most recently, the 2002 IEEE Cledo Brunetti Award and the 2002 Semiconductor Research Corporation Technical Achievement Award for his work with his colleague, S. Datta, on nanoscale electronics.